Experimental two-phase heat transfer study of R245fa in horizontal mini-channels at high saturation temperatures

Marijn Billiet[1], Remi Revellin[2], Romain Charnay[2] and Michel De Paepe[1]

[1] Department of Flow, Heat and Combustion Mechanics, Ghent University, Sint-Pietersnieuwstraat 41, 9000 Ghent, Belgium
[2] INSA-Lyon, CETHIL, CNRS, UMR5008, F-69621 Villeurbanne, France

E-mail: marijn.billiet@ugent.be

Abstract. Heat transfer measurements for R254fa were conducted. The heat transfer coefficient was determined for a smooth stainless steel tube with an inner tube diameter of 3 mm. The experiments were conducted for three heat fluxes (10, 30 and 50 W/m^2), five mass fluxes (100, 300, 500, 700 and 1000 $kg/(m^2 \cdot s)$) and at three saturation temperatures (40 °C, 70 °C and 125 °C). The experimental data was used to determine the influence of the saturation temperature, mass flux, heat flux and vapour quality on the heat transfer coefficient. At a low saturation temperature, the heat transfer coefficient increases with an increasing mass flux. However, at a high saturation temperature the heat transfer coefficient decreases with an increasing mass flux. Furthermore, the heat transfer coefficient increases with increasing vapour quality at a low saturation temperature. On the contrary, the heat transfer coefficient decreases at higher saturation temperatures.

1. INTRODUCTION

The use of Organic Rankine Cycles (ORCs) can help us to reduce the global CO_2-emissions. ORCs convert low-grade heat into mechanical energy. Some typical applications of ORCs are waste heat recovery and producing electricity of geothermal energy, solar energy or biomass [1, 2]. An ORC is a Rankine cycle which uses an organic fluid instead of steam. A typical example of an organic fluid used in ORCs is R245fa [3, 4].

A Rankine cycle consists of 4 components: a pump, an evaporator, an expander and a condenser. The pump pressurises the liquid working fluid. This pressurised liquid is then evaporated at a high temperature in the evaporator. Next, the organic vapour is expanded over the expander which produces mechanical energy. Finally the vapour is condensed in the condenser. In order to size the evaporator of an ORC correctly, a good heat transfer correlation is needed. If the evaporator is not sized correctly, this will either impair the ORC's performance or increase the construction cost.

In literature a large variety of heat transfer correlations exist [5, 6, 7]. Each correlation is based on experimental data within a certain range of working conditions. Hence, it is not certain if the correlation will work outside this range. Charnay et al. [8] compared his experimental results (R245fa) with existing heat transfer correlations. None of the tested existing heat

transfer correlations could predict the heat transfer coefficient very well at the high saturation temperatures relevant for ORCs.

The aim of this work is to present unpublished experimental heat transfer measurements of R245fa in a tube with an inner diameter of 3 mm. Further the influence of the saturation temperature, mass flux, heat flux and vapour quality on the heat transfer coefficient was analysed.

2. EXPERIMENTAL SETUP

The experimental setup and its verification is described more detailed in [9, 10]. A short summary is given here for completeness. The experimental setup was designed to test R245fa at ORC-conditions.

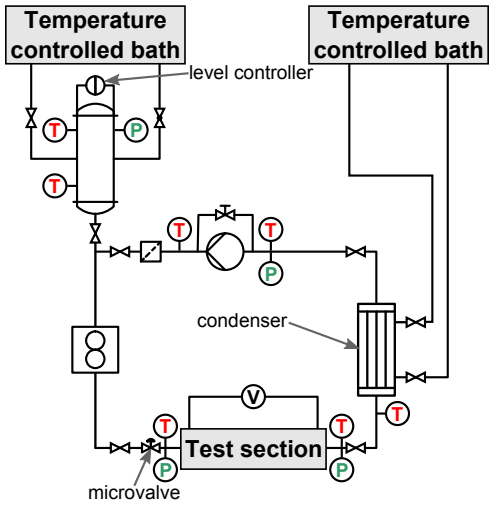

Figure 1. A schematic representation of the experimental setup.

Figure 1 shows a schematic representation of the experimental setup. The R245fa is consequently pumped through a filter/dryer, a Coriolis flowmeter, a micro-valve, a test section and a condenser. The micro-valve is used to avoid oscillation when boiling starts in the test section. Furthermore, the mass flow is controlled by the micro-valve together with a frequency-controlled pump and a bypass valve. The circuit also contains a temperature controlled reservoir which allows to set the saturation pressure inside the experimental setup. The whole experimental setup is controlled by a computer using Labview.

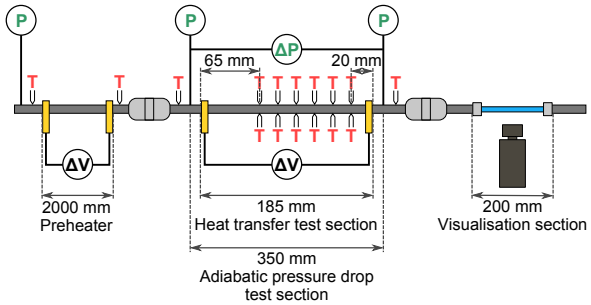

Figure 2. A detailed schematic diagram of the test section.

Figure 2 shows a detail of the test section. The test section consists of a preheater, an evaporator and a visualisation section. The preheater heats up the subcooled liquid to the required vapour quality. The preheater is a 2000 mm-long spirally-shaped stainless steel tube. The actual heat transfer and adiabatic pressure drop measurements are conducted in the evaporator. The evaporator is a 185 mm-long stainless steel tube. The inner and outer diameter of both tubes are respectively 3.00 mm and 5.99 mm. Both the preheater and the evaporator are heated using the Joule effect. To electrically insulate both sections from each other and the rest of the circuit, PEEK-resin tubes are used to connect the tubes. The temperatures at the in- and outlet of the preheater are measured by two K-type thermocouples ($D_j = 0.5$ mm). The bottom- and top-wall temperatures are measured at six position along the evaporator by K-type thermocouples ($D_j = 80$ m). The same thermocouples are also used to measure the top-wall temperature at the in- and outlet of the evaporator. The differential pressure over the evaporator is measured by 3 in-range-overlapping pressure sensors.

The visualisation section at the end of the test section is used to visually determine the flow regime using a high speed camera. The images are post-processed using a Matlab algorithm. The glass tube has respectively an inner and outer diameter of 2.96 mm and 5.95 mm.

Table 1. Overview of the experimental uncertainty of the experimental setup.

Parameter		TestRange	Uncertainty
d_i	[mm]	3	±0.03
d_o	[mm]	5.99	±0.03
L_{evap}	[mm]	185	±0.1
q_{ph}	[kW/m^2]	0.5 - 20	±1.2 - 5.6 %
q_{evap}	[kW/m^2]	10 - 55	±2.2 - 4.6 %
T_{sat}	[°C]	40 - 125	±0.3 - 0.8
G	[kg/(m^2·s)]	100 - 1500	±2 %
x	[-]	0 - 1	±0.001 - 0.03%
α	[kW/(K·m^2]	0.6 - 27.6	±max: 36 % avg: 17 %

The experiments where conducted with R245fa for five mass fluxes (100, 300, 500, 700 and 1000 kg/(m^2·s)), three heat fluxes (10, 30 and 50 W/m^2) and at three saturation temperatures (40 °C, 70 °C and 125 °C).

The error propagation used in this work is based on the book of Taylor [11]. An overview of the experimental uncertainty of the measurements is given in table 1.

3. RESULTS AND DISCUSSION

3.1. Definition of Heat Transfer Coefficient

In literature, two ways of reporting the average heat transfer coefficient exist:

$$\bar{\alpha}_1 = \frac{\dot{q}}{\bar{T}_{wall} - T_{sat}} \tag{1}$$

$$\bar{\alpha}_2 = \text{mean}\left(\frac{\dot{q}}{T_{wall} - T_{sat}}\right) \tag{2}$$

Most authors prefer equation 1 to define the average heat transfer coefficient. In equation 1, $\bar{T}_{wall}$ is the average wall temperature measured around the perimeter (e.g. the mean of the temperature measured at the top and the bottom of the tube wall). Other authors [12] average out the different local heat transfer coefficients determined at the perimeter (equation 2).

In most cases, both definition give similar results considering the uncertainty. However, when the difference between the wall temperatures at different positions around the perimeter increases, the results of both definitions start to deviate significantly. Furthermore, when the temperature difference between the wall and the saturated fluid decreases, the deviation gets larger. Hence, in the case of stratified flows or partial dry-out it is important to know which definition is used when the results from literature are used to construct a correlation. In this work, equation 1 is used to report the average heat transfer coefficient.

3.2. Stratification at high saturation temperatures

For small tube diameters, stratification of the two phases is often suppressed [13] due to the large capillary force. The Eötvös number (Eo) given in equation 3 is commonly used to express stratification.

$$Eo = \frac{(\rho_l - \rho_g)\, g d_i^2}{\sigma} \tag{3}$$

The Eötvös number expresses the ratio of the gravitational force to the surface tension force. For R245fa, the Eötvös number increases rapidly starting from a saturation temperature of 110 °C. During the experiments, stratification also occurred at high saturation temperatures as seen in

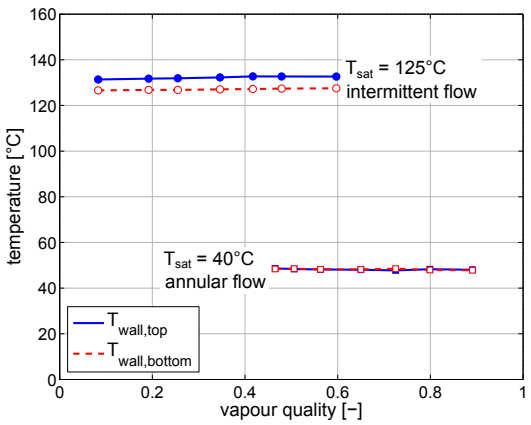

Figure 3. The wall temperature measured at the top and bottom of the tube as a function of the vapour quality for different saturation temperatures. The heat flux at the wall is 54 kW/m^2 and the mass flux is 100 kg/(m^2·s). (circle = intermittent flow; square = annular flow)

figure 3. Due to the stratification, there is a much thinner liquid film at the top of the tube. This thin film suppresses nucleate boiling which is a very important factor at high heat fluxes and low mass fluxes. Hence, the top tube wall temperature is much higher than the bottom wall temperature due to the lower local heat transfer coefficient.

3.3. Influence Saturation Temperature

In general the heat transfer coefficient increases with increasing saturation temperature as shown in figure 4a. However, if the mass flux, heat flux and vapour quality are all very high (see figure 4b) the heat transfer coefficient decreases with increasing saturation temperature.

With increasing saturation temperature, the vapour density increases, the liquid density decreases and the surface tension decreases for R245fa. This results in an increasing contribution of nucleate boiling to the total flow boiling heat transfer due to a decreasing bubbles detachment radius and an increasing number of nucleation sites [14]. Hence, more bubbles will be formed and they will detach faster from the wall surface, enhancing the nucleate boiling heat transfer.

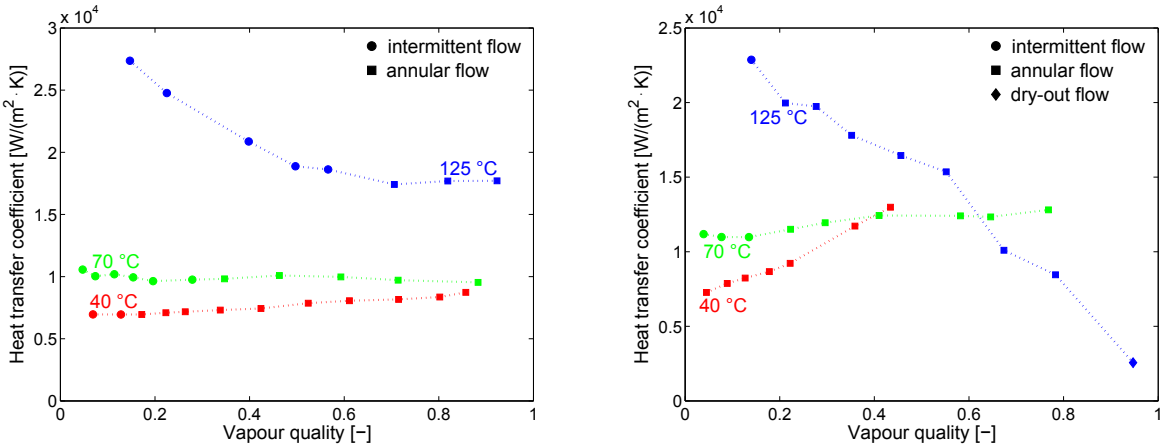

(a) G =300 kg/(m^2·s) (b) G =700 kg/(m^2·s)

Figure 4. The heat transfer coefficient as a function of the vapour quality for different saturation temperatures and a heat flux of 54 kW/m^2.

Moreover, the decrease of vapour density with increasing saturation temperature reduces the flow velocities, reducing the convective contribution to the heat transfer. In general one can conclude that the nucleate boiling heat transfer mechanism gains in dominance with increasing saturation temperature.

At low saturation temperatures, in general the heat transfer coefficient increases with increasing vapour quality but at high saturation temperatures the opposite is noticed. Hence, the increase of the heat transfer coefficient with increasing saturation temperature is larger for lower vapour qualities.

The increase in vapour quality, increases the flow speed and thus enhances the convective heat transfer. However, an increase in vapour quality also thins the the annular liquid film and decrease the wall superheat. Hence, this lead to a decreasing number of active nucleation sites [15]. This explains the different influence of the vapour quality at low and high saturation temperature where the heat transfer is respectively dominated by convection and nucleate boiling.

3.4. Influence Heat Flux

Figure 5a, 5b and 6 show that in general the heat transfer coefficient increases with increasing heat flux in the pre-dry-out region. Due to the higher heat flux, the contribution of nucleate boiling increases. During dry-out the liquid film at the wall disappears and thus also the heat transfer due to nucleate boiling. This explains also the sudden drop in figure 6.

In general, the increase of the heat transfer coefficient with heat flux also reduces with increasing vapour quality. At higher vapour qualities, the convective heat transfer mechanism becomes more dominant and the nucleate boiling mechanism is reduced. Hence, at high vapour qualities there is a smaller effect of the heat flux on the heat transfer coefficient.

In figure 5a (low mass flux), the nucleate boiling is the dominant heat transfer mechanism because the heat transfer coefficient does not change significantly with the vapour quality. The increasing vapour quality thins the liquid layer at the wall which reduces the number of nucleations sites due to an decrease in wall superheat. On the other hand, the contribution of the convective heat transfer mechanism increases but this increase is not large enough to compensate at higher saturation temperatures were nucleate boiling is dominant.

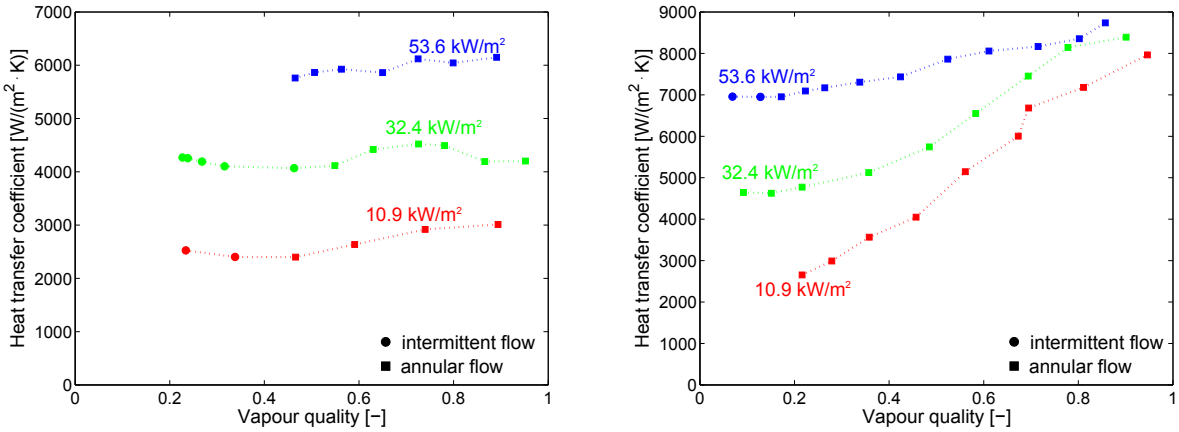

(a) G =100 kg/(m^2·s) (b) G =300 kg/(m^2·s)

Figure 5. The heat transfer coefficient as a function of the vapour quality for different heat fluxes at saturation temperature of 40 °C.

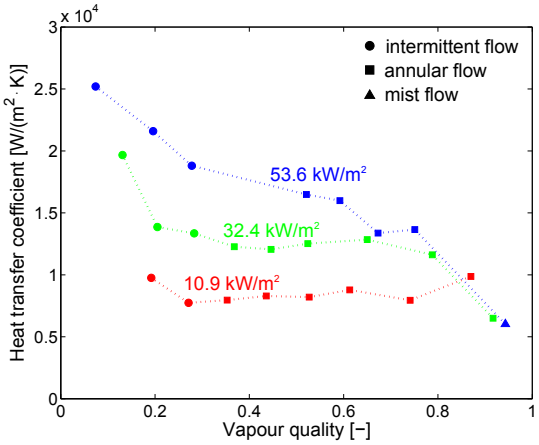

Figure 6. The heat transfer coefficient as a function of the vapour quality for different heat fluxes at saturation temperature of 125 °C and a mass flux of 500 kg/(m^2·s).

3.5. Influence Mass Flux

Figure 7a and 7b show the influence of the mass flux on the heat transfer coefficient at respectively a low (40 °C) and high (125 °C) saturation temperature. At the low saturation temperature (figure 7a), the heat transfer coefficient increases with increasing mass flux. However, the opposite is noticed at a high saturation temperature (figure 7b). Furthermore, at a low saturation temperature, the increase with increasing mass flux gets larger for increasing vapour quality. In contrary, at a high saturation, the opposite is noticed.

Previous results suggest that the main heat transfer mechanism is respectively convection and nucleate boiling at a low and a high saturation temperature. The same conclusion was also found by Charnay *et al.* [10].

An increasing mass flux and vapour quality results in a increase of the flow velocity. Furthermore, the liquid film becomes thinner with increasing vapour quality. Both the increased flow velocity and the lower thermal resistance of the liquid film result in a increase of convective heat transfer. On the other hand, the thinner liquid film also lowers the superheat of the liquid

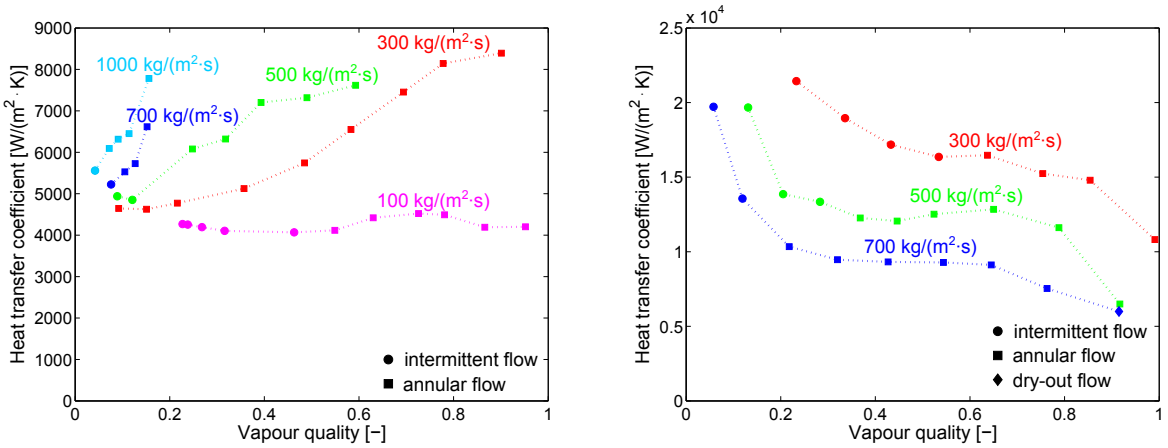

(a) T_{sat} =40 °C (b) T_{sat} =125 °C

Figure 7. The heat transfer coefficient as a function of the vapour quality for different mass fluxes and a heat flux of 32 kW/m^2.

film which is adversely for nucleate boiling [16, 17].

When nucleate boiling is the dominant heat transfer mechanism, the increase of the convective contribution to the heat transfer cannot compensate for the decrease of the nucleate boiling contribution.

3.6. Influence Vapour Quality

At low saturation temperature (figure 5b), an increase of the heat transfer coefficient is noticed with increasing vapour quality due to the increase of convection. However at a high saturation temperature (figure 6), the heat transfer coefficient decrease with increasing vapour quality. The increasing vapour quality suppresses the nucleate boiling which is the dominant heat transfer mechanism at high saturation temperatures.

At low saturation temperatures, the heat transfer coefficient increases more strongly with increasing vapour quality if the mass flux increases. However, at high saturation temperatures, the combined effect of vapour quality and mass flux is not noticeable except in the intermittent flow regime (figure 7b).

4. CONCLUSION

This work presented unpublished experimental heat transfer measurements of R245fa in a tube with an inner diameter of 3 mm and discussed the influence of the saturation temperature, mass flux, heat flux and vapour quality on the heat transfer coefficient.

The heat transfer coefficient respectively increased and decreased with an increasing mass flux at a low and high saturation temperature. Furthermore, the heat transfer coefficient increased with increasing vapour quality at a low saturation temperature. On the contrary, the heat transfer coefficient decreased at higher saturation temperatures. Hence, the influence of vapour quality and mass flux on the heat transfer coefficient is dependent of the saturation temperature.

Existing heat transfer models for R245fa are based on experimental data measured at low saturation temperatures. This explains why none of the existing heat transfer correlation Charnay et al. [8] tested, worked well for predicting their results at high saturation temperatures.

Acknowledgments
Research funded by a Ph.D. grant (nr. 141733) of the Agency for Innovation by Science and Technology (IWT)

References

[1] Tchanche B F, Lambrinos G, Frangoudakis A and Papadakis G 2011 *Renewable and Sustainable Energy Reviews* **15** 3963–3979
[2] Wang E H, Zhang H G, Fan B Y, Ouyang M G, Zhao Y and Mu Q H 2011 *Energy* **36** 3406–3418
[3] Lecompte S, Huisseune H, van den Broek M and De Paepe M 2015 *Energy* **87** 60–76
[4] Saleh B, Koglbauer G, Wendland M and Fischer J 2007 *Energy* **32** 1210–1221
[5] Kattan N, Thome J R and Favrat D 1998 *Journal of Heat Transfer* **120** 156–165
[6] Li W and Wu Z 2010 *International Journal of Heat and Mass Transfer* **53** 1778–1787
[7] Kanizawa F T, Tibiri C B and Ribatski G 2016 *International Journal of Heat and Mass Transfer* **93** 566–583
[8] Charnay R, Revellin R and Bonjour J 2015 *International Journal of Heat and Mass Transfer* **87** 653–672
[9] Charnay R 2014 *Experimental Study of Flow Boiling in Horizontal Minichannels at High Saturation Temperature* PhD dissertation Institut National des Sciences Appliquées de Lyon URL `http://theses.insa-lyon.fr/publication/2014ISAL0047/these.pdf`
[10] Charnay R, Revellin R and Bonjour J 2015 *International Journal of Heat and Mass Transfer* **87** 636–652
[11] Taylor J R 1997 *An Introduction to Error Analysis: The Study of Uncertainties in Physical Measurements* 2nd ed (University Science Books) ISBN 978-0-935702-75-0
[12] Tibiriá C B and Ribatski G 2010 *International Journal of Heat and Mass Transfer* **53** 2459–2468
[13] Coleman J W and Garimella S 1999 *International Journal of Heat and Mass Transfer* **42** 2869–2881
[14] Gorenflo D, Chandra U, Kotthoff S and Luke A 2004 *International Journal of Refrigeration* **27** 492–502
[15] Dang C, Haraguchi N and Hibara E 2010 *International Journal of Refrigeration* **33** 655–663
[16] Cioncolini A and Thome J R 2010 *International Journal of Multiphase Flow* **36** 293–302
[17] Ducoulombier M, Colasson S, Bonjour J and Haberschill P 2011 *Experimental Thermal and Fluid Science* **35** 597–611